

Spatial-temporal Variation and Local Source Identification of Air Pollutants in a Semi-urban Settlement in Nigeria Using Low-cost Sensors

Oyediran Kayode Owoade¹, Pelumi Olaitan Abiodun¹,
Opeyemi R. Omokungbe¹, Olusegun Gabriel Fawole^{1,2},
Felix Samuel Olise¹, Olalekan O.M. Popoola³, Roderic L. Jones³,
Philip K. Hopke^{4,5*}

¹ Environmental Pollution Laboratory, Department of Physics and Engineering Physics, Obafemi Awolowo University, Ile-Ife, Nigeria

² Atmospheric Science Unit, Department of Environmental Sciences, Stockholm University, Stockholm, Sweden

³ Department of Chemistry, University of Cambridge, Cambridge, UK

⁴ Institute for a Sustainable Environment, Clarkson University, Potsdam, NY, USA

⁵ Department of Public Health Sciences, University of Rochester School of Medicine and Dentistry, Rochester, NY, USA

ABSTRACT

Low-cost sensors were deployed at five locations in a growing, semi-urban settlement in southwest Nigeria between June 8 and July 31, 2018 to measure particulate matter (PM_{2.5} and PM₁₀), gaseous pollutants (CO, NO, NO₂, O₃ and CO₂), and meteorological variables (air temperature, relative humidity, wind speed and wind-direction). The spatial and temporal variations of measured pollutants were determined, and the probable sources of pollutants were inferred using conditional bivariate probability function (CBPF). Hourly PM_{2.5} and PM₁₀ concentrations ranged from 20.7 ± 0.7 to 36.3 ± 1.6 µg m⁻³ and 47.5 ± 1.5 to 102.9 ± 5.6 µg m⁻³, respectively. Hourly gaseous pollutant concentrations ranged from 348 ± 132 to 542 ± 200 ppb CO, 21.5 ± 7.2 ppb NO₂ and 57.5 ± 11.3 to 64.4 ± 14.0 ppb O₃. Kruskal-Wallis ANOVA on ranks determined statistically significant spatial differences in the hourly-average pollutant concentrations. Diel variation analyses indicated that CO₂, PM_{2.5}, and PM₁₀ peaked in the early hours of most days, O₃ at noon while NO, NO₂, and CO peaked in the evening. Most pollutants were of anthropogenic origins and exhibited the highest contributions from the southwest at most sampling locations. There were strong similarities between pollutants source contribution at two of the monitoring sites that were in residential areas with a frequently used paved road. Mitigation strategies need to be established to avoid further deterioration of ambient air quality that negatively affect public health.

Keywords: Temporal variation, Low-cost sensors, Particulate matter, CBPF, Source identification

1 INTRODUCTION

Environmental degradation is a major consequence of increasing population, economic development, rapid industrialization, and technological advancement (Morais *et al.*, 2012; Mohsin *et al.*, 2019). Air pollution is a well-known global problem in developed and developing nations due to its effects on public health and the environment at local, regional, and continental scales. Air pollution heightens the risk of respiratory and cardiovascular diseases, lowers the survival rates in the newborns, reduces the life expectancy of people with existing health issues, and produces acute effects on the exposed population (Dockery *et al.*, 1993; Dockery and Pope, 1994; Pope, 2000). Clean air is a basic requirement for human comfort, health, and well-being and is being

OPEN ACCESS

Received: October 19, 2020

Revised: July 11, 2021

Accepted: July 18, 2021

* **Corresponding Author:**


phopke@clarkson.edu

Publisher:

Taiwan Association for Aerosol
Research

ISSN: 1680-8584 print

ISSN: 2071-1409 online

 **Copyright:** The Author(s).
This is an open access article distributed under the terms of the [Creative Commons Attribution License \(CC BY 4.0\)](https://creativecommons.org/licenses/by/4.0/), which permits unrestricted use, distribution, and reproduction in any medium, provided the original author and source are cited.



affected by air pollution, leading to human morbidity and mortality. Environmental issues such as acid rain, visibility impairment, alteration of the atmospheric radiation budget, and modification of cloud properties are also adverse effects of air pollution (Owoade *et al.*, 2012; Tian *et al.*, 2014). Air pollutants have been studied from both human and environmental health perspectives. Regulatory and advisory bodies such as the United States Environmental Protection Agency (U.S. EPA) and the World Health Organization (WHO) have established standards/guidelines for daily and annual concentrations of the different air pollutants. However, these values are exceeded in many locations.

Air pollutants may arise from natural or anthropogenic sources, and they can be transported over long distances, crossing both local and international boundaries (Owoade *et al.*, 2012; Fawole *et al.*, 2016). The major atmospheric pollutants include sulfur dioxide (SO₂), oxides of nitrogen (NO/NO₂/NO_x), ozone (O₃), oxides of carbon (CO/CO₂) and particulate matter (PM). PM is particularly important because of its variable chemical composition, size, morphology, frequent occurrences of high concentrations, and its significant effects on human health and the environment (Sumesh *et al.*, 2017). Ozone is formed in the troposphere through photochemical reaction of NO_x and volatile organic compounds (VOCs) (Seinfeld and Pandis, 2016). Significant sources of NO in urban settings are motor vehicles and power generation systems (Ul-Haq *et al.*, 2015). NO_x is primarily emitted as NO with a smaller proportion of NO₂. However, the reaction with O₃ rapidly converts NO to NO₂. The CO concentrations found in the lower atmosphere are typically associated with incomplete combustion activities as well as the oxidation of atmospheric methane.

In addition to the variable strength of the emission sources, variations in air pollutant concentrations are associated with the meteorological conditions, local environmental properties (land area, size, vegetation cover and population), and the availability of other pollutant precursors (Khiem *et al.*, 2010; Wang *et al.*, 2018). Notable spatial and temporal variations have been found for CO within the boundary layer up to scales of high inter hemispheric gradients (Yashiro *et al.*, 2009). PM concentrations at any location vary with the local source strengths and other processes such as atmospheric chemical reactions, deposition, precipitation, and new particle formation (Sumesh *et al.*, 2017). Hu *et al.* (2018) and Zhang and Jiang (2018) reported that local emission sources and potential effects of meteorology at meso - and synoptic scales might influence PM concentrations. The mixing layer depth and local weather dynamics drive the dispersion of source emissions at local scales while long-range transport affects the movement of PM over regional, transboundary, and continental scales. Multiple authors (Owoade *et al.*, 2012; Guttikunda and Gurjar, 2012; Jayamurugan *et al.*, 2013; Cheng *et al.*, 2013; Gogikar and Tyagi, 2016; Gogikar *et al.*, 2018) reported that meteorological variables such as wind speed and direction, air temperature, relative humidity, and rainfall govern the advection and dispersion of pollutants in any region.

A major challenge in monitoring air pollutant concentrations across an area and the influence of meteorology is the availability of measurement instruments. Most federal reference method (FRM or research grade) instruments are costly and difficult to move because of their size, power requirements, and ancillary systems such as sampling manifolds. Thus, they are typically stationed in fixed locations (Karagulian *et al.*, 2019). Data obtained from the FRMs yield limited information on spatial variations of pollutants. Recent improvements in micro-technology have led to the development of portable monitoring systems for particulate matter and gaseous pollutants. These monitors are low-cost, very mobile, and can be deployed indoors and outdoors (Kumar *et al.*, 2015; Sousan *et al.*, 2016; Manikonda *et al.*, 2016; Zikova *et al.*, 2018; Crilley *et al.*, 2018; Masiol *et al.*, 2018; Li *et al.*, 2020).

Existing studies of particulate air pollution in this area of Ile-Ife, Nigeria focused on the elemental characterization and receptor modeling to identify the likely particulate pollutant sources (Ogundele *et al.*, 2016; 2017; Owoade *et al.*, 2015). The only major point source in the area is a scrap steel and iron smelting facility (Owoade *et al.*, 2015; 2016; Ogundele *et al.*, 2017). Owoade *et al.* (2016) identified four sources in both the PM_{2.5} and PM_{2.5-10} size fractions that were labeled: soil (44%), savannah burning (26%), scrap processing (18%), and vehicular emissions (12%) for PM_{2.5} and soil plus biomass burning (71%), sea salt (22%), scrap processing (5%) and vehicle emissions (including tire wear) (2%) for PM_{2.5-10}. The biomass burning in the PM_{2.5} fraction would likely also include cooking emissions that include both the biomass burning for heat and the emitted cooking particles. All of these measurements were made either adjacent to the iron/steel



facility or on the Obafemi Awolowo University campus. Thus, limited information was available on the PM concentration variability across the area and its influencing factors.

If the temporal and spatial variability and directional characteristics of the pollutants can be determined, they can be employed to identify hot spots, pollutant sources and provide the information needed to implement appropriate mitigation measures. Therefore, this study monitored particulate matter and gaseous pollutants concentrations in Ile Ife, Nigeria, analyzed their temporal variations and spatial variability, and provided directional information of their measured concentration using low-cost sensors. Omokungbe *et al.* (2020) made an initial report of the PM_{2.5} and PM₁₀ results in which they examined the relationships between the measured PM values with temperature and relative humidity values. Higher PM concentrations were observed at lower temperatures and there was no variation of PM with RH when the RH < 80%. There were effects of RH for values > 80% likely due to the hygroscopic growth of the particles above the likely deliquesce relative humidity value. However, detailed spatial and temporal analyses were not made and those analyses and the resulting information about gaseous and particulate pollutions is the focus of this work.

2 METHODOLOGY

2.1 Study Area

The study was conducted in a fast-growing city, Ile-Ife in southwestern Nigeria (7.33°N and 4.31°E, 294 m A.S.L.). It has an average population of about 502,000 (NPC, 2006) that was projected to have grown to 886,300. A major road passes through the city with several minor roads (paved and unpaved) linking different parts of the city for the easy movement of vehicles and passengers. The city hosts Obafemi Awolowo University (OAU), Obafemi Awolowo University Teaching Hospital Complex (OAUTHC), and a private polytechnic college. In addition to these institutions, a steel smelting factory is situated on the outskirts of the city along the Ife-Ibadan Expressway. Climatically, it experiences two major seasons (wet and dry). The dry season occurs from November to March the following year while the rainy season runs from April to October. During the dry season, there is little precipitation with high solar radiation, clear sky conditions, and high air temperatures. Cold, dust-laden northeasterly trade winds from the Bodele Depression in the Chad Basin in the Sahara Desert can blow across the region delivering significant quantities of dust for several days. In the wet season, the near surface flow is controlled by southwesterly winds emanating from the Atlantic Ocean and resulting into moderate temperatures and an abundance of rainfall (Falaiye *et al.*, 2013).

2.2 Air Monitoring

Gaseous pollutants (CO, CO₂, NO, NO₂, and O₃) and size segregated particulate matter fractions (PM_{2.5} and PM_{2.5-10}) were monitored using low-cost monitoring sensors in a monitoring package at five locations in Ile Ife, southwestern Nigeria. The sampling locations were distributed across the city and the choices of the location were considered appropriate based on open space and the absence of any obstruction that would hinder the free circulation of air. Three sites (P1, P2 and P3) were located within the Obafemi Awolowo University campus, and two locations (P4 and P5) were within a fast-growing residential area of the city with one location generally downwind of an industrial area situated very close to the busy Ife-Ibadan Expressway. Fig. 1 shows the sampling site locations in the city. The five low-cost sensor packages were simultaneously deployed at all the chosen locations. Each low-cost monitor was placed 3 m above the ground level. Brief descriptions of each site are presented in Table 1. Air monitoring took place from June till July 2018. The duration was short as this is a preliminary study on air quality research in southwestern Nigeria.

The sensor packages used in this study were AlphaSense low-cost portable air monitoring devices. Optical particle counters (OPC-N2) measured particulate matter while gaseous pollutants were monitored with electrochemical sensors. The OPC sensor records particles per milliseconds in 16 size bins and estimates PM concentrations in the range of 0.38 to 17 microns with a maximum particle count of 10000 s⁻¹ (Crilley *et al.*, 2018). The OPC-N2 converts the particle concentration to mass concentration corresponding to the PM metrics: PM_{2.5} (for particulate matter ≤2.5 μm) and PM₁₀ (for particulate matter ≤10 μm). The electrochemical sensors operate on amperometric

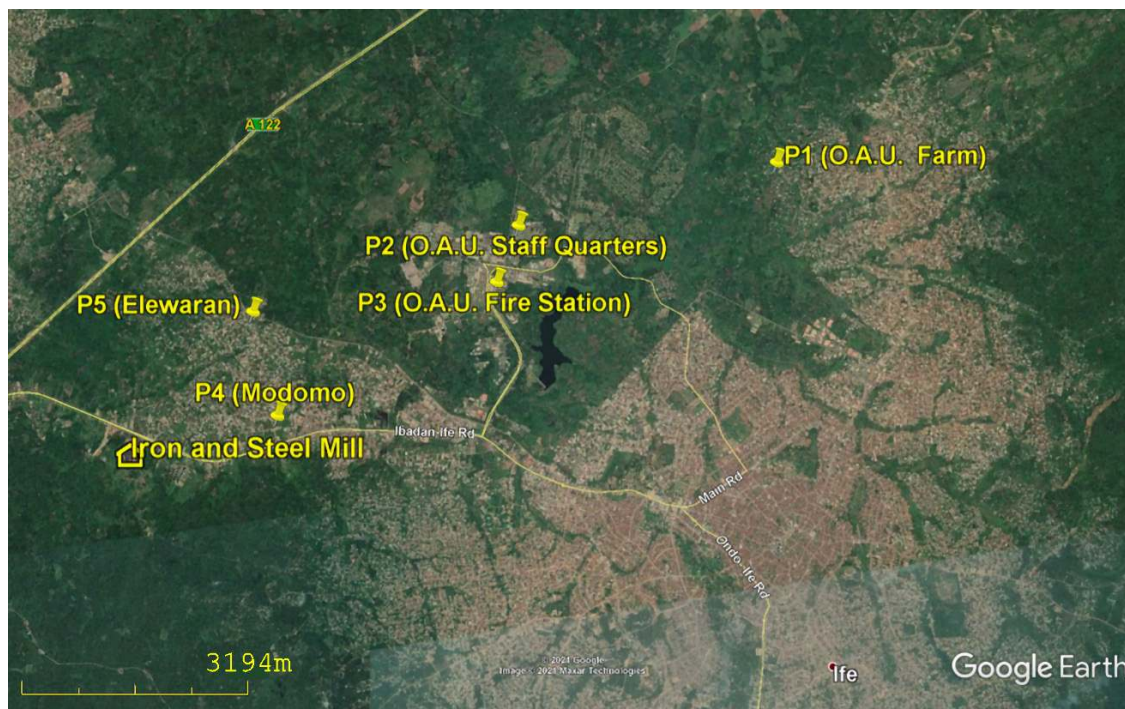


Fig. 1. Location of monitoring sites and the scrap iron and steel mill.

Table 1. Description of monitoring sites.

Code	Sites	Site Description
P1	Teaching and Research Farm (OAUTF)	Within OAU farm and it is dedicated to agricultural activities including planting and rearing of animals.
P2	Staff Quarters	Within OAU Staff used residential area and close proximity to the university waste dumpsite.
P3	Fire Service Station	Within OAU campus area near the university main road and close proximity to a bus station.
P4	Modomo	Fast growing residential area, close to the main road and downwind of iron and steel smelting factory.
P5	Elewaran	Residential area further away from iron smelter and major road, closer to a minor road.

sensor principles that sense selected toxic gases at the parts per-million-level in an environment. Each unit also has temperature and relative humidity (RH) sensors as well as a 2-D sonic anemometer to measure wind speed and directions. Further details of the fundamental principles and operational procedures of the sensor and associated atmospheric variables sensors were given by Popoola (2012) and Popoola *et al.* (2016, 2018) for the gaseous sensors. The PM sensor has been evaluated by Sousan *et al.* (2016), Crilley *et al.* (2018), Chatzidiakou *et al.* (2019), and Li *et al.* (2020). Mead *et al.* (2013), Popoola *et al.* (2018) and Chatzidiakou *et al.* (2019) present extensive comparisons of these monitors to reference monitoring systems during field studies in the United Kingdom.

The major advantages of this sensor include low cost, low power use, high sensitivity, fast response, selectivity, multiple species monitoring, near real time measurement, and simple operating procedures (Popoola, 2012; Popoola *et al.*, 2018). At each site, a box containing the sensor nodes were mounted at about 3 m above the ground on a 6 m pole and powered with a rechargeable battery. The low-cost sensors were operated simultaneously at the five sites for two months (June 8–July 30, 2018 in the wet season). The sensors recorded the gaseous and PM concentrations, and the meteorological variables every second and stores 20 s averages of these parameters. For the continuous measurements, the data were retrieved from a universal serial



board (USB) stick every two weeks and then underwent further processing with suitable computer packages and software developed by the Department of Chemistry, University of Cambridge, UK. The PM mass concentrations and meteorological data were averaged to hourly values and further statistical analyses were performed using the Openair R software package (Carslaw, 2015; Carslaw and Ropkins, 2012) and SigmaPlot V14.

2.3 Statistical Analysis

The summary statistics were calculated. Normality was tested under the hypothesis: H_0 : there is no normal distribution pattern with data obtained from the study area to determine to use either parametric or non-parametric methods. The confidence intervals for this study were set at 95% such that p -values ≤ 0.05 resulted in the acceptance of the null hypothesis. The normality test was the Kolmogorov-Smirnov test. Spatial variations in the measured variables were assessed using the Kruskal-Wallis analysis of variance (ANOVA) on ranks (Kruskal and Wallis, 1952) with confidence level set at 95% under the hypothesis that there was spatial variation (median values were not equal) in pollutant concentrations and meteorological parameters observed across the monitoring sites. Dunn's method (Dunn, 1964) was used to compare the site to site (pairwise comparison) variation at a 95% confidence level.

2.4 Source Directionality Using Conditional Bivariate Probability Function

The directional dependence of local sources of PM affecting each sampling sites was explored with conditional probability function (CPF) embedded in a bivariate polar plot (BPP) using the conditional bivariate probability function (CBPF). Bivariate polar plots provide information on the potential source influences by wind speed and direction on the receptor site. The CBPF estimates the probability that high pollutant concentrations (above a predetermined threshold value) are associated with a given wind direction and speed (Kim *et al.*, 2003; Uria-Tellaetxe and Carslaw, 2014; Sumesh *et al.*, 2017). It is based on the ratio of the number of samples in a wind sector and wind speed interval with concentrations greater than the given threshold to the total number of samples in that sector and wind speed interval. The CBPF values were calculated using Eq. (1):

$$CBPF_{\Delta\theta, \Delta u} = \frac{m_{\Delta\theta, \Delta u | c > x}}{n_{\Delta\theta, \Delta u}} \quad (1)$$

where $m_{\Delta\theta, \Delta u}$ is the number of samples with wind direction from a given $\Delta\theta$ and wind speed interval in the interval of Δu having a concentration c greater than a threshold x and $n_{\Delta\theta, \Delta u}$ is the total number of samples of that combination of wind speed and direction intervals ($\Delta u, \Delta\theta$). In this study, x was set at the 75th percentile.

2.5 Coefficient of Divergence

Coefficient of divergence (CoD) is a parameter used for the evaluation of degree of divergence of two datasets. This analysis was performed to understand the variability or degree of uniformity of pollutants species measured simultaneously in two sites during a specified period. The CoD was evaluated as follows:

$$CoD_{jk} = \sqrt{\frac{1}{p} \sum_{i=1}^p \left(\frac{x_{ij} - x_{ik}}{x_{ij} + x_{ik}} \right)^2} \quad (2)$$

where j and k represents the paired sampling sites; x_{ij} and x_{ik} stands for the average concentration for the same pollutants at the two sites and p is the number of pollutants under study. CoD is known to be self-normalizing and can be obtained from short and long-term averages (Wongphatarakul *et al.*, 1998). CoD values range from zero to unity where values close to zero reveals strong similarity between the two sites while values close to unity depicts between the sites (Wongphatarakul *et al.*, 1998; Liu *et al.*, 2017). Wilson *et al.* (2005) reported that CoD values of 0.2 were consistent with spatial homogeneity of air pollutants.



2.6 Coefficient of Variation

The Coefficient of Variation (CoV or r-squared) was also used to assess the spatial variation of pollutant species between sites. The r-squared values shows the variance of a pollutant in a site that can be explained by the pollutants at another site. Like CoD, r-squared values range from 0–1. The r-squared values greater or equal to 0.7 suggests strong similarity in the pollutant temporal variations between the compared sites while values closer to zero suggests significant difference in the pollutant variation between the sites.

3 RESULTS AND DISCUSSION

3.1 Average Hourly Concentration of the Measured Pollutants

The results of the average (\pm standard deviation) of the concentration of the measured pollutants at the five sites are presented in Table 2. The maximum 1-hour average concentration for PM_{2.5} and PM₁₀ are 36 ± 1.5 and $111 \pm 14 \mu\text{g m}^{-3}$ (P4), respectively. The high PM concentrations can be attributed to the location of this site in the fast-developing residential area with unpaved roads and a smelting industry. PM_{2.5}/PM₁₀ ratios have been used to aid source identification (Gogikar *et al.*, 2018). In this study, moderate values of PM_{2.5}/PM₁₀ ratio were found at P5, P2, and P4, (0.44, 0.43 and 0.43 respectively) showing high anthropogenic contributions to the PM concentrations at these sites likely including suspended dust from the roads. A previous study on the Obafemi Awolowo University campus using gravimetric methods reported daily mean PM_{2.5} and PM₁₀ mass concentrations of 25.4 ± 2.4 and $37.2 \pm 32.4 \mu\text{g m}^{-3}$ (Owoade *et al.*, 2012) were lower than the mass concentration obtained in this study, but with a much higher PM_{2.5}/PM₁₀ ratio. The daily average PM₁₀ mass concentrations in this study exceeded the $50 \mu\text{g m}^{-3}$ limit value recommended by the WHO. Also, the daily average values of PM₁₀ were 2.0, 1.8 and 1.6 times the threshold limit values of $50 \mu\text{g m}^{-3}$ stipulated by EU (2014) at P1, P4, and P3, respectively.

The maximum one-hour average CO concentration was 542 ppb at P3 that was attributed to its proximity to a busy road. The vehicular emissions and other anthropogenic activities like cooking with solid fuels (Obaseki *et al.*, 2017) contributed to the values observed at this site. NO maximum concentration of hourly average was 7.34 ppb at site P3, similar to the value of CO. Ul-Haq *et al.* (2015) associated concentration of NO in cities to vehicular emission. The minimum average concentration of CO₂ was found at P3 (428 ppm) and the maximum was 471 ppm at P4. The maximum hourly concentration of NO₂ occurred at P4 (21.5 ppb), an area downwind of an industrial plume while the lowest concentration was found at the farm settlement (13.7 ppb). The highest ozone concentration was found at P4 (64.4 ppb). These results showed that maximum hourly-mean concentrations of PM_{2.5}, PM₁₀, CO₂, O₃ and NO₂ were observed at P4, a fast-growing residential area and downwind of a smelting industry. The range of concentrations of O₃, NO and NO₂ observed in this study were similar to those reported by Hagenbjörk *et al.* (2017) at three different sites (regional, traffic and background) in Sweden.

Table 2. Descriptive statistics of hourly averages of measured pollutants.

	Site	P1	P2	P3	P4	P5	WHO	EPA-NAAQS	EU
	Averaging period	Mean \pm SE	Mean \pm SE	Mean \pm SE	Mean \pm SE	Mean \pm SE			
CO*	1-hour	393 \pm 69	365 \pm 69	542 \pm 200	348 \pm 132	404 \pm 121			
CO ₂ **	1-hour	465 \pm 39	429 \pm 23	428 \pm 22	4713 \pm 37.9	465 \pm 37			
NO*	1-hour	4.6 \pm 5.9	6.5 \pm 5.9	7.3 \pm 7.2	7.2 \pm 7.1	6.5 \pm 5.2			
NO ₂ *	1-hour	13.7 \pm 5.9	15.3 \pm 7.0	19.8 \pm 7.6	21.5 \pm 7.2	17.5 \pm 6.0			
O ₃ *	1-hour	58.8 \pm 5.4	57.5 \pm 11.3	63.7 \pm 10.9	64.4 \pm 14.0	59.4 \pm 12.1			
PM _{2.5} ***	1-hour	35.1 \pm 1.2	20.7 \pm 0.7	31.4 \pm 1.0	36.3 \pm 1.6	21.0 \pm 1.0			350
PM ₁₀ ***	1-hour	103 \pm 5.5	47.5 \pm 1.5	80.4 \pm 2.4	111 \pm 14	50.3 \pm 3.5			
PM _{2.5} /PM ₁₀	1-hour	0.37	0.43	0.37	0.43	0.44			
PM _{2.5}	24-hour	35.5 \pm 3.0	21.0 \pm 1.3	31.7 \pm 2.1	36.5 \pm 3.7	21.1 \pm 2.5	25	35	
PM ₁₀	24-hour	104 \pm 8.9	47.8 \pm 2.4	80.9 \pm 4.0	109 \pm 26.5	51.4 \pm 7.9	50	150	50
PM _{2.5} /PM ₁₀	24-hour	0.37	0.44	0.39	0.43	0.44			

* ppb; ** ppm; *** $\mu\text{g m}^{-3}$.



3.2 Observed Meteorology during the Study Period

The descriptive statistics for the meteorological variables (temperature, relative humidity and wind speed) at the five sites are presented in Table S1. Mean (\pm SD) temperature across the sites ranged from $23.4 \pm 3.7^\circ\text{C}$ (P2) to $25.6 \pm 3.2^\circ\text{C}$ (P5). The Kruskal-Wallis test indicated a statistically significant differences ($p < 0.05$) in temperature across the sites except for P1/P3, P2/P3, and P4/P5. The mean (\pm SD) of hourly relative humidity ranged from $74.9 \pm 16.0\%$ (P2) to $79.9 \pm 15.7\%$ (P3). There was a statistically significant difference in the hourly average relative humidity observed across the monitoring sites ($p < 0.05$) except for P1/P5. The hourly averaged wind speed range across study sites was 0.05 to 2.48 m s^{-1} . The Kruskal-Wallis analysis of the hourly mean wind speeds indicated statistically significant differences ($p < 0.05$) except P1/P2 and P3/P5. Given that these sites are in built areas, it is likely that local surface obstructions are diverting the wind and potentially reducing the observed speeds. Low wind speeds during calm period limit the dispersion of emissions within a locality leading to increased pollutant concentration (Dai *et al.*, 2020).

The prevailing wind directions shown in Fig. S1 reflect winds primarily from the southwest with some northwesterly and limited southeasterly flows. Calm winds were observed about 16.7% of the time. There were prevailing low wind speeds that aided pollutant accumulation. It can be seen that there are some notable differences among the sites with P4 and P5 having northwesterly winds than at the other sites. P1/P2 and P1/P5 are the only pairs that have similar median directions.

3.3 Spatial Variation of Pollutants

The distributions of hourly-averaged concentration of the pollutants at the five monitoring sites are presented in Fig. 2 as box and whisker plots. The result showed the median (black line within the box), 25th and 75th percentiles of the pollutants. The lower and upper whiskers showed the minimum and maximum pollutant's concentration during the study. The results of the detailed statistical analyses are presented in Tables S1 and S2 of the Supplemental Information file. Those results are summarized in Table S3.

CO had the largest interquartile range and thus, its highest variation at site P3. Generally, there were significant differences in CO across all sites. This pattern could be attributed to a variety of activities including open burning and vehicular emissions. The highest concentrations of CO being at P3 could be attributed to its location near a bus park. For CO₂, there were significant differences among most of the sites. However, P1/ P5 and P2/ P3 did not have significant differences. P1 is at the farm at one end of the domain while P5 is at the other end of the domain and is closest to the Iron and steel mill and in the residential district. P2 and P3 are quite close to one another with no significant sources that could affect these two sites differently.

There were significant differences in the variation of NO across most of the study area. However, the Dunn's result showed that there were again no statistically significant differences between the two sites within the university (P2 and P3). Similar periods of cooking and associated burning activities were likely to occur within the residential areas. Significant differences in the O₃ and NO₂ concentrations were also found across most of the sites. Sites P1 and P2 did not differ for either the NO₂ or O₃ medians. O₃ medians did differ between P1/P5, P2/P4, and P2/P5. P4 and P5 are likely to be more highly affected by the major road south of the residential area, local combustion, and possibly emissions from the iron and steel mill.

There were also significant differences in PM_{2.5} and PM₁₀ values across most of the study sites. Greater variability in the particulate matter fractions were observed at P4, a residential area with many unpaved roads and extensive two-wheel motor vehicle transport. For both fractions, it was observed that there were no significant differences observed between P1 and P3. P2 and P4 also had similar PM₁₀ median values although P4 had a much greater range of values.

3.4 Temporal Variation of Gaseous and Particulate Matter Pollutants

3.4.1 Diel variations

The diel variations of CO concentration (Fig. 3) had two major peaks that occurred in the morning (06:00–08:00 hr) and at night (18:00–20:00 hr). The variation shown in the plots provides the 5th and 95th confidence intervals represented by the shaded areas. These times are

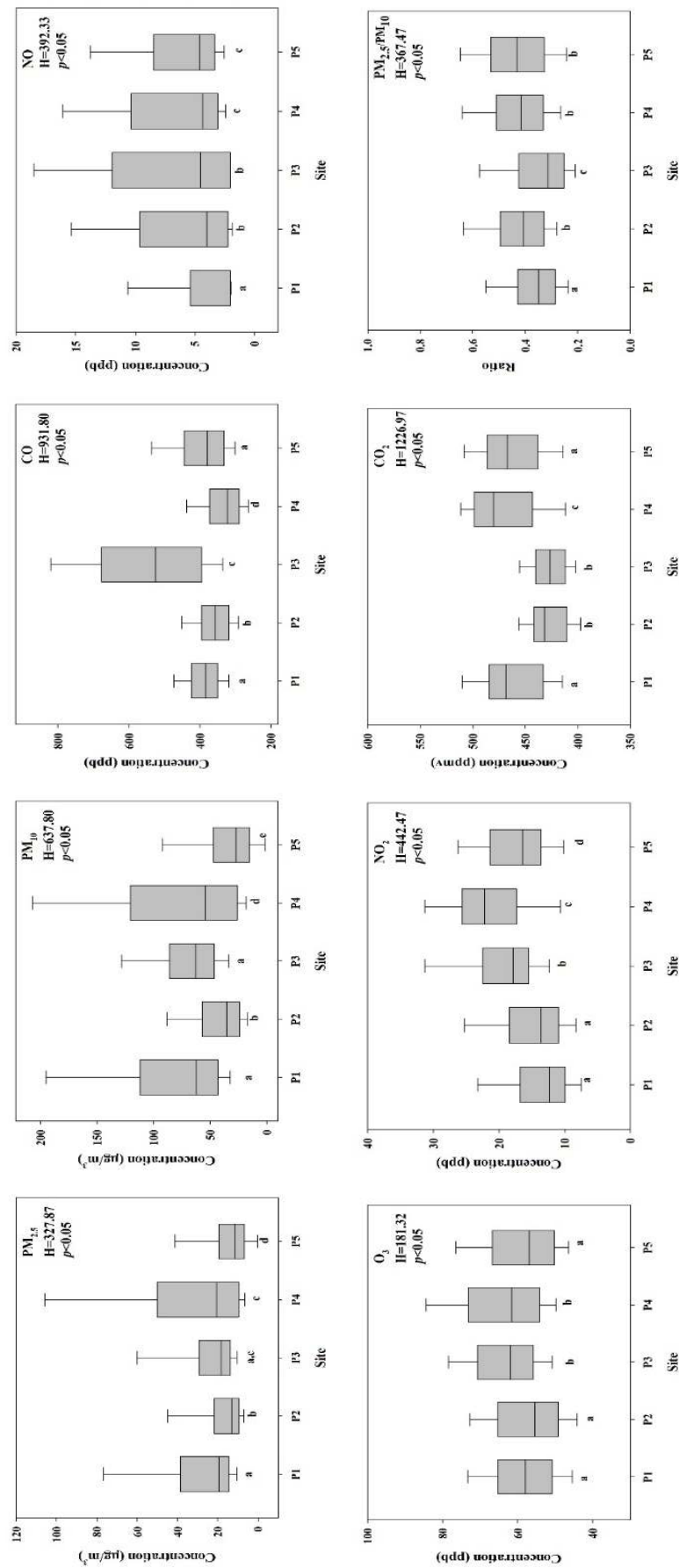


Fig. 2. Spatial variation of pollutants across the study sites using Kruskal Wallis One-way analysis of variance with pairwise comparison using Dunn's method. Similar alphabets represent similarity in the variation of the pollutants at the sites. Confidence interval set at 95%.

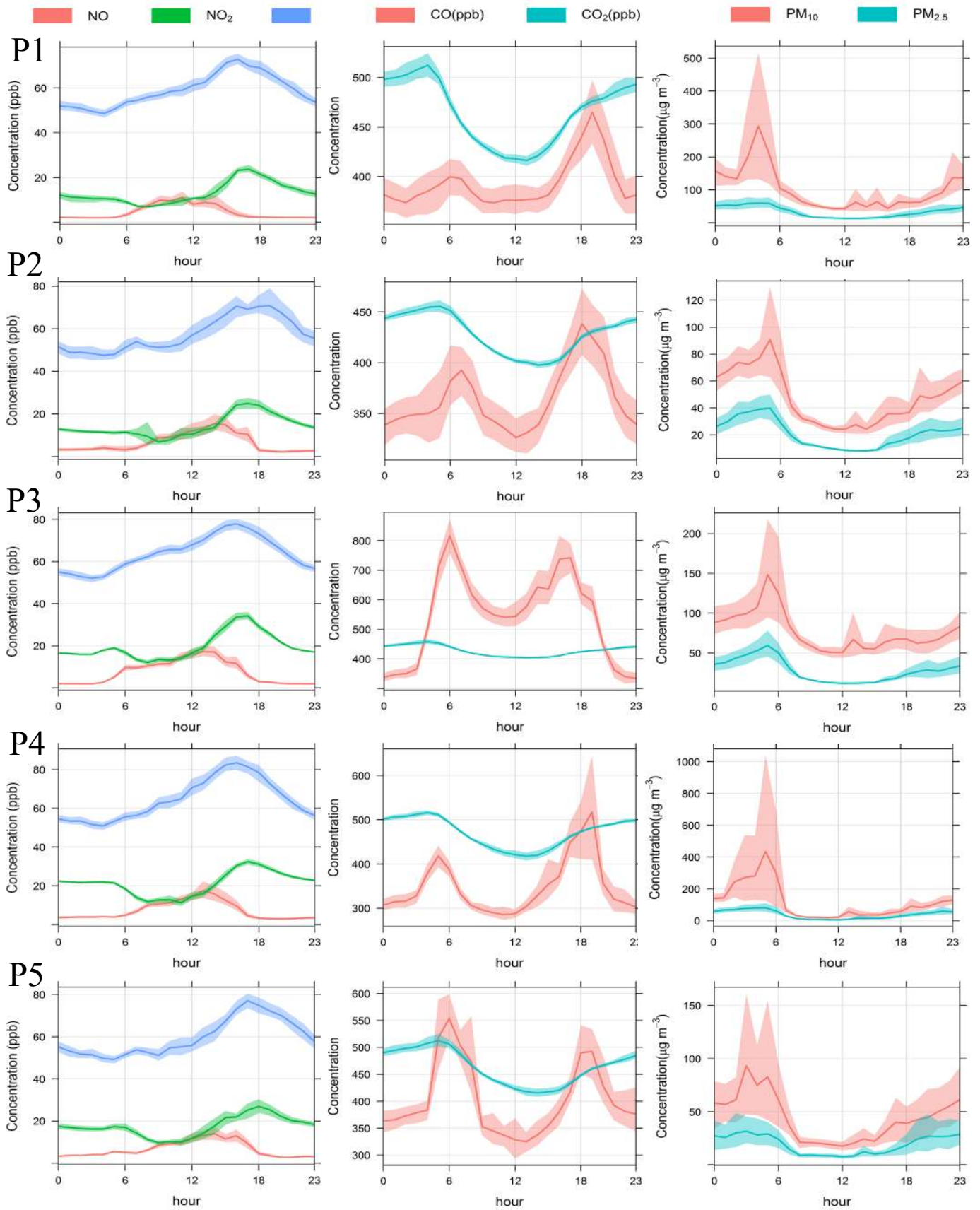


Fig. 3. Diel variation of CO (ppb), CO₂ (ppm), NO (ppb), NO₂ (ppb), O₃(ppb), PM_{2.5} (µg m⁻³) and PM₁₀ (µg m⁻³) at P1 to P5.



typically periods of higher traffic volumes (P3 and P5) while domestic combustion and electricity generators are mostly used at night at P2 and P4. Thus, these sources likely drive this observed variation. Higher morning peaks were observed at P3 and P5 while the higher peaks at the other locations (P1, P2, and P4) occurred in the evening. The diel variations of CO₂ were similar across the study area. Boundary layer dynamics and source emission patterns are the major factors that influence the variability of CO₂ concentration (Wang *et al.*, 2010; Fang *et al.*, 2016). The hourly peaks observed for CO and CO₂ at all locations peaked in the evening when local biomass burning for cooking were likely driving the observed patterns. There was a secondary CO peak in the morning likely from morning cooking.

The diel variations of NO, NO₂, and O₃ (Fig. 3) at the monitoring sites were very similar to one another. There was an increase in NO from early morning 03:00 hr until 14:00–15:00 hr. NO peaked prior to the peak of NO₂ and O₃ which showed that photochemical transformation of NO through titration by ozone until the NO was sufficiently low that ozone concentrations could rise (Wang *et al.*, 2018).

The similitude in the temporal variations can probably be attributed to general combustion (transport and residential combustion emissions) in the study area. The concentration of NO₂ decreased during the convective hours (12:00–15:00 hr) of the day when mixing and secondary pollutant formation was maximal but dilution and vertical transport of primary pollutants predominated. The particulate matter fractions (PM_{2.5} and PM₁₀) showed similar diel variations (Fig. 3) at all stations with a major peak at 05:00–06:00 hr except at P5 that peaked earlier than the other stations. P4 and P5 are close to the iron and steel smelting factory where its major operations take place at night (6:00 pm–5:00 am). Unlike these sites, P4 and P5 had two peaks between midnight and 06:00 hr that could represent the time for batch processes of the factory's operation. Additionally, the PM_{2.5} and PM₁₀ temporal variation in the study area can be assumed to be influenced by atmospheric dispersion playing significant role in transporting the pollutants from the source to the sites.

3.5 Day of the Week Variation of Pollutants

The day of week variations (Fig. S2) showed that CO exhibited similar daily variations at all locations. There were higher concentrations during the weekdays than on the weekends (Saturday and Sunday) for most sites. P3 showed the largest drop in CO concentration on weekends. This reduction was expected because it was close to a major university road that was used less on weekends. CO₂ followed a similar variation pattern at all the monitoring stations. Unlike CO, CO₂ concentration increased on weekend days (Saturday and Sunday) compared to weekdays. This result may reflect people not working and thus present at their residences as well as additional cooking being done.

The daily concentration of NO₂ ranged from 10 to 20 ppb during the study and showed a uniform temporal variation at the sites. There were no differences in the day of week variations of NO and O₃ at the monitoring sites. The day of week variations of PM_{2.5} and PM₁₀ at the monitoring sites were similar. This result could be due to similar sources, largely transportation and the transport of particles from iron and steel smelting factory at few kilometres from the sites. For most of the sites, the highest PM concentrations were observed midweek (Tuesday and Wednesday).

3.6 Source Identification and Characterization

3.6.1 Conditional bivariate probability plots

Fig. 4 shows the CBPF results for CO. The residential area sites (P4 and P5) show opposite directions at relatively low wind speeds mostly under 2 m s⁻¹ suggesting that local activities in this area are the primary sources. Given that the winds are generally from the southwest (Fig. S1), there is clearly substantial local emissions. These sources would include the minor road bordering the area and local combustion for cooking. P1 shows the highest probabilities in the southwesterly direction toward the campus area for wind speeds under 1.5 m s⁻¹. P2 and P3 on the OAU campus again show preferred southerly directions. P2 appears to be seeing emissions from the road and the area around the Fire Station whereas P3 is affected by the campus area to the south southwest to the west southwest.

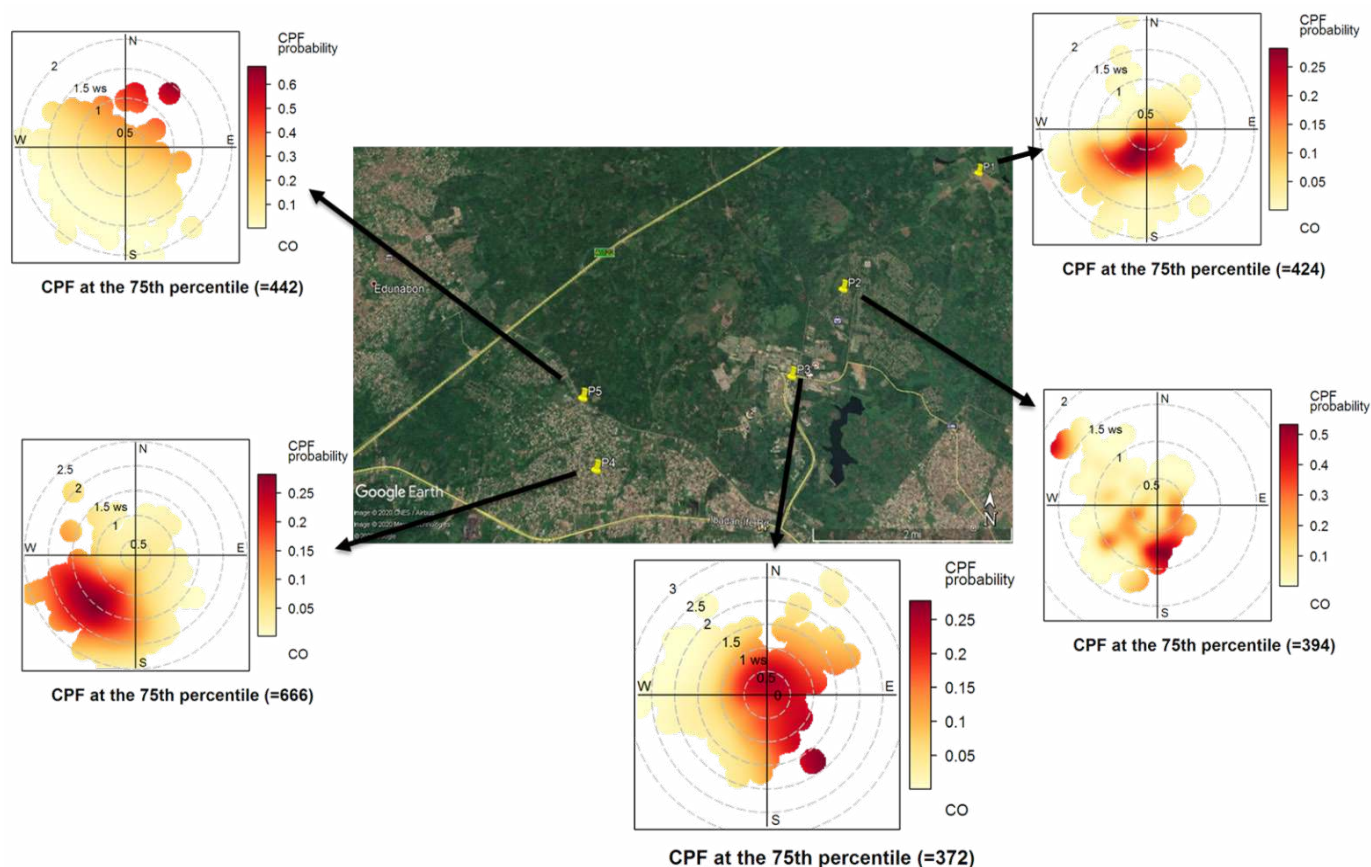


Fig. 4. Conditional Bivariate Probability Functions for CO (ppb) for sites P1–P5.

Fig. 5 presents the CBPF plots for CO₂. They have very different patterns than those observed for CO with all of the higher probability areas appearing at higher wind speeds. There are much smaller relative variations in the CO₂ concentrations since local emissions are superimposed on the ~400 ppm global background. P1 showed a strong influence to the southwest under higher wind speeds (~5 m s⁻¹), a lower probability area to the southeast under lower wind speeds, some influence from the north at speeds between 2.0 and 2.5 m s⁻¹, and at very little low wind speed probabilities. Thus, there are none or very weak sources in the immediate vicinity of P1. There are large residential areas to the southwest to the southeast (city of Ife). Sources affecting P2 are on the OAU campus area to the west southwest. P3 shows a weaker influence from the campus area and a strong focused area to the east southeast. A large source is the Obafemi Awolowo University Teaching Hospitals Complex (OAUTHC) that is 4.8 km from P3 at 97.5°. They would be cooking using LPG as well as drawing considerable traffic in the area. Another smaller potential source is the Moremi High School is 2.5 km at 96.9° from P3. However, there is no cooking done there and food is brought in as needed.

Figs. 6 and 7 show the CBPF plots for PM_{2.5} and PM₁₀. All these plots show that the highest probabilities for high concentrations occur when wind speeds are low (typically < 1 m s⁻¹). The P3 plot suggests influence from the road that curves around the Fire Station building. However, directionality is not well defined at low wind speeds. Thus, the differences in patterns observed between P2 and P3 may not be as substantial as it appears. The P4 plot suggests emissions in the residential area even with only weak flows from the westerly and northerly directions. The P5 plot also points to the residential area, but again all under low wind speed conditions. Neither the P4 or P5 plots suggest an effect of the iron and steel mill. The only obvious difference between the two size fraction plots is at P3 where the PM₁₀ plot shows areas of influence to the northwest and east southeast at higher wind speeds.

The CBPF plots for NO, NO₂, and O₃ are provided in Figs. S3–S5. There are notable differences between the NO and NO₂ plots suggesting that NO is more local in origins while NO₂ is

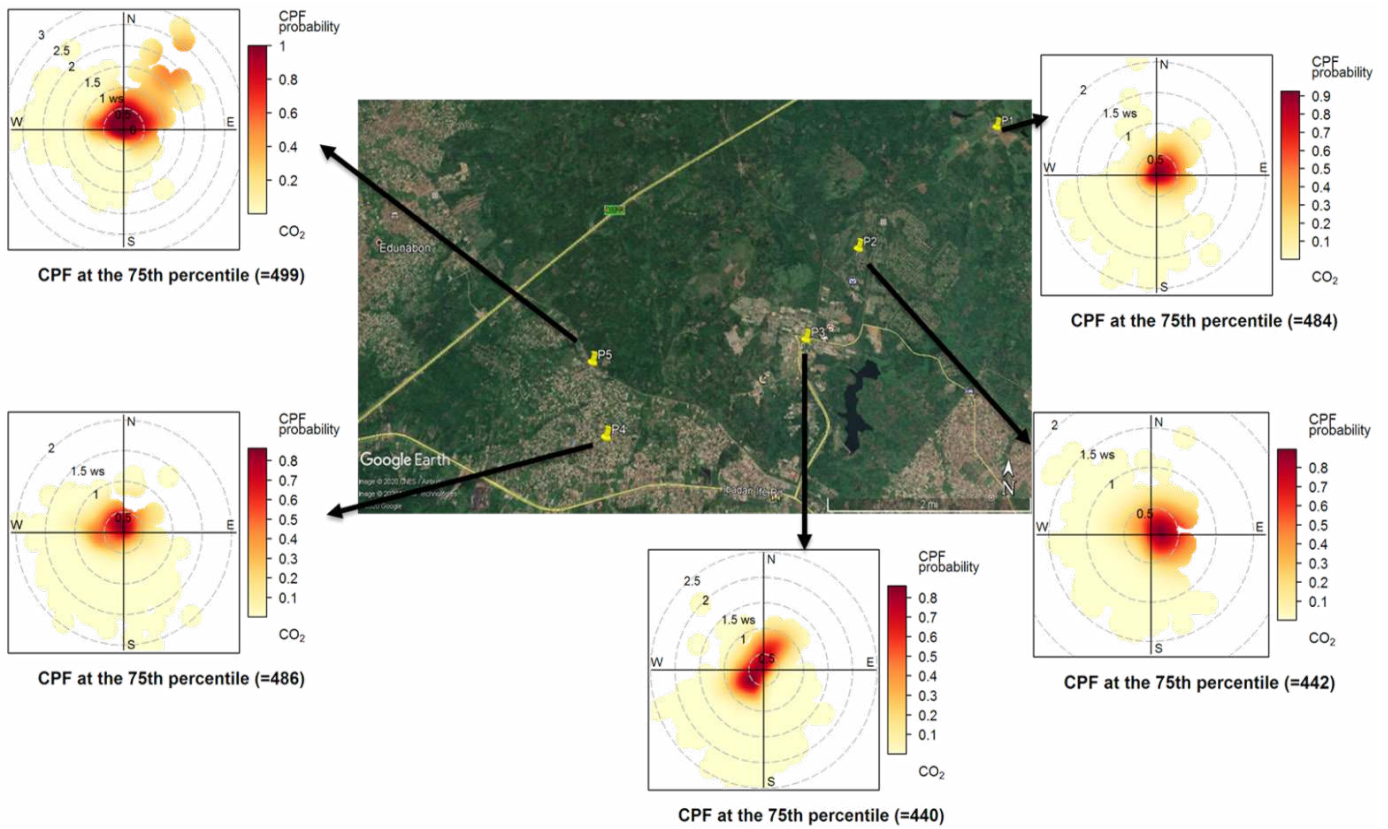


Fig. 5. Conditional Bivariate Probability Functions for CO₂ (ppm) at sites P1–P5.

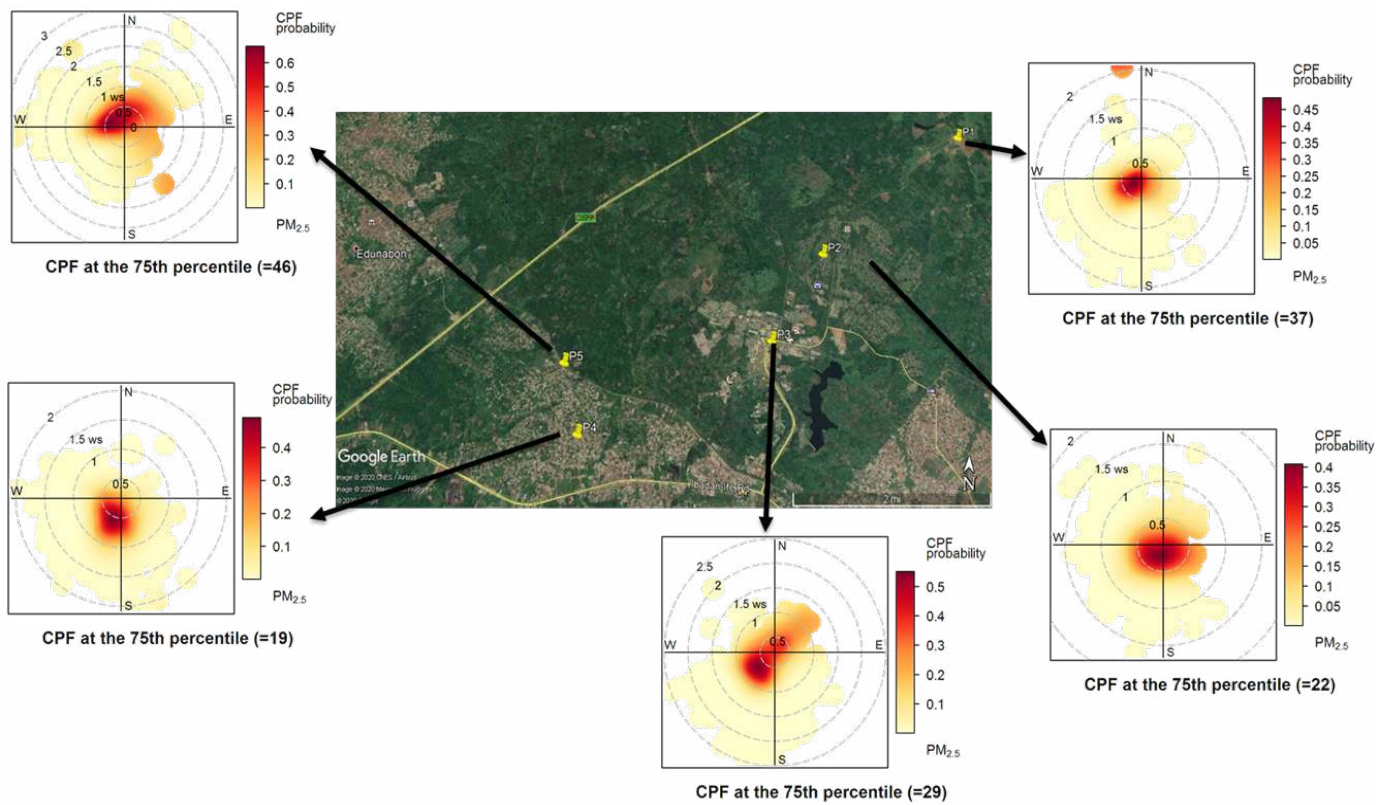


Fig. 6. Conditional Bivariate Probability Functions for PM_{2.5} ($\mu\text{g m}^{-3}$) at sites P1–P5.

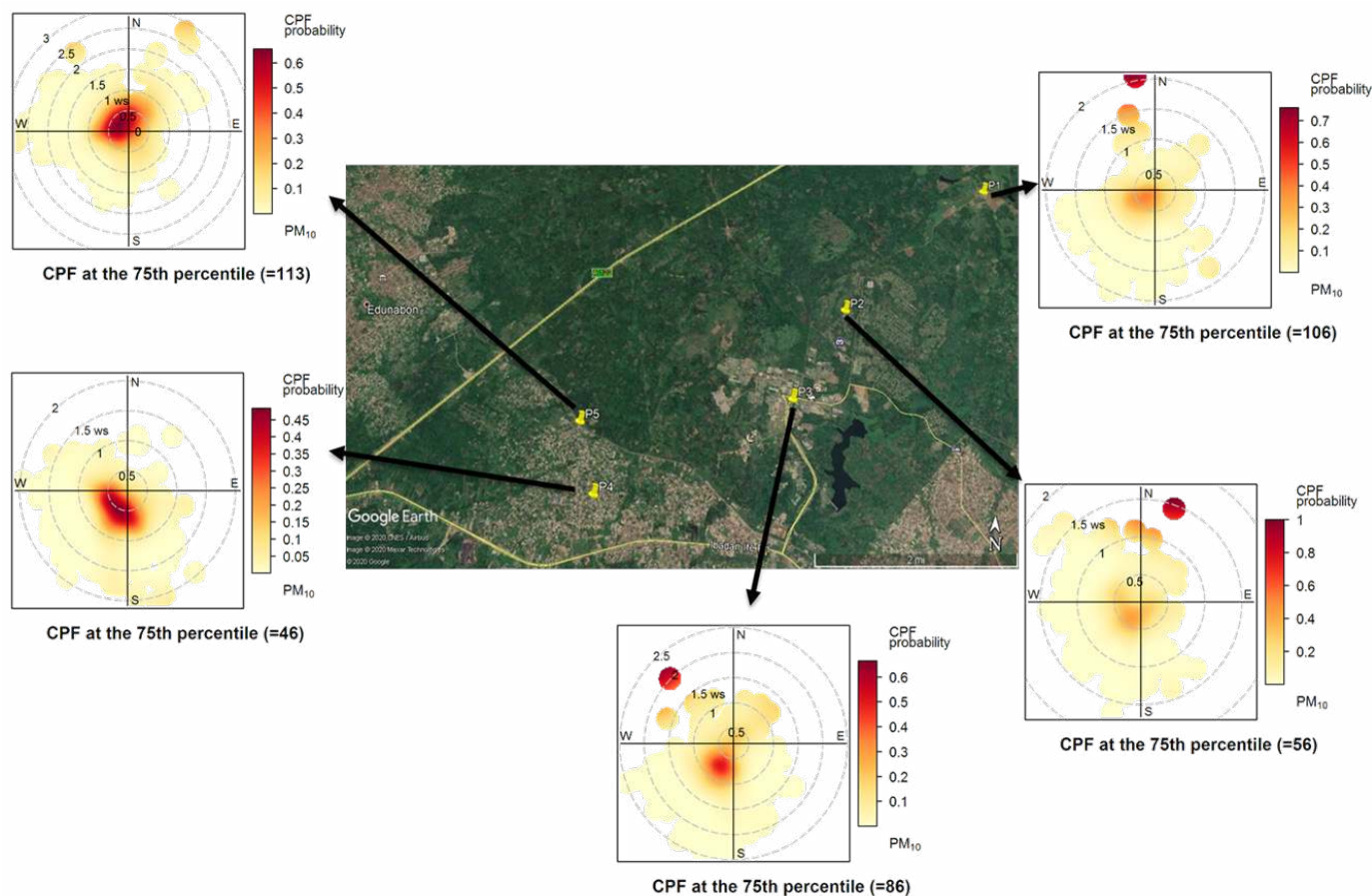


Fig. 7. Conditional Bivariate Probability Functions for PM₁₀ ($\mu\text{g m}^{-3}$) at sites P1–P5.

transported. At P4, there is a strong node to the SW at higher wind speeds that may reflect the high temperature combustion occurring at the iron and steel mill. The P2 plot shows a likely influence of combustion sources on the OAU campus such as cooking with LPG that did not affect P3. P3 again shows an NO area to the ESE (Fig. S4) similar to those seen in the O₃ and PM₁₀ plots at higher wind speeds suggesting a source that is likely to be the OAUTHC. Most of the high probability areas in the NO₂ plots are at higher wind speeds around the outside of the plots similar to the O₃ plots (Fig. S5). These patterns suggests that NO₂ and O₃ are likely in photolytic steady-state and then interact with the local NO emissions to reduce the ozone concentrations. However, the NO titration does not produce sufficient NO₂ relative to the transported concentrations to produce high probabilities at low wind speeds (Wang *et al.*, 2018).

3.6.2 Coefficients of divergence

The CoD values are presented in the Table 3. CoD values < 0.2 are considered similar in concentration values (Wilson *et al.*, 2005). The most similar sites were P2 and P5. These sites are the residential areas near a heavily travelled paved road. Overall, there were similarities among

Table 3. Coefficients of Divergence among the monitoring sites.

Sites	P1	P2	P3	P4	P5
P1	0				
P2	0.18	0			
P3	0.14	0.16	0		
P4	0.33	0.37	0.33	0	
P5	0.18	0.04	0.13	0.36	0

Significant values (< 0.20) are bolded.



P1, P2, P3 and P5 compared with P4. P4 is characterized with unpaved roads and a dense residential population.

3.6.3 Coefficients of variance

The r-squared values are presented in Table 4. The variance of pollutants at most sites cannot be explained with by the same pollutant at the other sites except for CO₂ at P3 and P1 which are locations within the university and presence of sources of combustion within close proximity. This variation could also be influenced by prevailing meteorology of the study sites.

3.7 Limitations

Due to limited availability of the monitoring equipment, this study was only conducted over a 2-month period during the later spring and early summer. Thus, it does not reflect seasonal variations in emission or meteorological conditions. Given differences in wind directions, precipitation, and human activities over an entire year, this work only provides a snapshot of this period.

Table 4. Spatial r-squared values among the measured pollutants.

Pollutant	Site				
		P2	P3	P4	P5
CO	P1	0.008	0.067	0.004	0.000
	P2		0.006	0.000	0.015
	P3			0.047	0.001
	P4				0.017
	P5				
NO	P1	0.238	0.468	0.325	0.115
	P2		0.135	0.138	0.092
	P3			0.378	0.224
	P4				0.178
	P5				
O ₃	P1	0.100	0.599	0.178	0.122
	P2		0.040	0.221	0.216
	P3			0.220	0.028
	P4				0.077
	P5				
NO ₂	P1	0.356	0.599	0.545	NA
	P2		0.143	0.154	0.032
	P3			0.263	0.058
	P4				0.285
	P5				
CO ₂	P1	0.354	0.757	0.551	0.284
	P2		0.281	0.494	0.511
	P3			0.545	0.260
	P4				0.355
	P5				
PM ₂₅	P1	0.109	0.350	0.158	0.004
	P2		0.099	0.118	0.018
	P3			0.138	0.023
	P4				0.108
	P5				
PM ₁₀	P1	0.150	0.260	0.151	0.009
	P2		0.030	0.130	0.059
	P3			0.029	0.001
	P4				0.114
	P5				



4 CONCLUSIONS

This study used low-cost sensor-based monitors to measure gaseous pollutants, PM, and meteorological variables within a fast-growing semi-urban settlement over a period of 8 weeks. The study found temporal and spatial variations of the pollutants across the study area. Wind in the study area had speeds from 0.5 to 2.5 m s⁻¹ mostly from the southwest suggesting sources in the identified wind direction. The observed spatial variations for each pollutant were statistically significant at a 95% confidence level. The diel variations of pollutants revealed that CO, CO₂, PM_{2.5} and PM₁₀ had two prominent peaks at morning and night times while NO, NO₂ and O₃ were observed to peak between 12:00–15:00 hr. Average daily concentration showed that all the pollutants peaked majorly during the weekdays (Tuesday or Wednesday) except CO₂ that generally peaked on Sunday. Local sources such as heating/cooking and traffic were likely major sources as well as the scrap processing factory to the SW of the study area. The area is a fast-growing semi-urban settlement with increasing urban development. Thus, there is a need to implement mitigation strategies to reduce local emissions of pollutants. Also, limiting emission sources to the southwest of the study area such as from the scrap processing plant could lower the pollution load across the study area.

SUPPLEMENTARY MATERIAL

Supplementary material for this article can be found in the online version at <https://doi.org/10.4209/aaqr.200598>

REFERENCES

- Carslaw, D.C. (2015). The openair manual—open-source tools for analysing air pollution data. Manual for version, 1, 1–4. <https://davidcarslaw.com/project/openair/>
- Carslaw, D.C., Ropkins, K. (2012). *openair* — an R package for air quality data analysis. Environ. Modell. Software 27–28, 52–61. <https://doi.org/10.1016/j.envsoft.2011.09.008>
- Chatzidiakou, L., Krause, A., Popoola, O.A.M., Di Antonio, A., Kellaway, M., Han, Y., Squires, F.A., Wang, T., Zhang, H., Wang, Q., Fan, Y., Chen, S., Hu, M., Quint, J.K., Barratt, B., Kelly, F.J., Zhu, T., Jones, R.L. (2019). Characterising low-cost sensors in highly portable platforms to quantify personal exposure in diverse environments. Atmos. Meas. Tech. 12, 4643–4657. <https://doi.org/10.5194/amt-12-4643-2019>
- Cheng, I., Zhang, L., Blanchard, P., Dalziel, J., Tordon, R. (2013). Concentration-weighted trajectory approach to identifying potential sources of speciated atmospheric mercury at an urban coastal site in Nova Scotia, Canada. Atmos. Chem. Phys. 13, 6031–6048. <https://doi.org/10.5194/acp-13-6031-2013>
- Crilley, L.R., Shaw, M., Pound, R., Kramer, L.J., Price, R., Young, S., Lewis, A.C., Pope, F.D. (2018). Evaluation of a low-cost optical particle counter (Alphasense OPC-N2) for ambient air monitoring. Atmos. Meas. Tech. 11, 709–720. <https://doi.org/10.5194/amt-11-709-2018>
- Dai, Q., Liu, B., Bi, X., Wu, J., Liang, D., Zhang, Y., Feng, Y., Hopke, P.K. (2020). Dispersion normalized PMF provides insights into the significant changes in source contributions to PM_{2.5} after the COVID-19 outbreak. Environ. Sci. Technol. 54, 9917–9927. <https://doi.org/10.1021/acs.est.0c02776>
- Dockery, D.J., Pope, C.A. (1994). Acute respiratory effects of particulate in air pollution. Ann. Rev. Public Health 15, 107–132.
- Dockery, D.W., Pope, C.A., Xu, X., Spengler, J.D., Ware, J.H., Fay, M.E., Ferris, B.G., Speizer, F.E. (1993). An Association between Air Pollution and Mortality in Six U.S. Cities. N. Engl. J. Med. 329, 1753–1759. <https://doi.org/10.1056/NEJM199312093292401>
- Dunn, O.J. (1964). Multiple comparisons using rank sums. Technometrics 6, 241–252. <https://doi.org/10.1080/00401706.1964.10490181>
- Falaiye, O.A., Yakubu, A.T., Aweda, F.O., Abimbola, O.J. (2013). Mineralogical characteristics of harmattan dust in Ilorin, Sub-sahara Africa. Ife J. Sci. 15, 175–181. <https://doi.org/10.4314/ijfs.v15i1>



- Fang, S., Tans, P.P., Steinbacher, M., Zhou, L., Luan, T., Li, Z. (2016). Observation of atmospheric CO₂ and CO at Shangri-La station: Results from the only regional station located at southwestern China. *Tellus B* 68, 28506. <https://doi.org/10.3402/tellusb.v68.28506>
- Fawole, O., Olofinjana, B., Owoade, O. (2016). Compositional and Air-mass Trajectory Analysis of a Heavy Dust Episode (HDE) Aerosols in Ile-Ife, Nigeria. *Br. J. Applied Sci. Technol.* 13, 1–15. <https://doi.org/10.9734/BJAST/2016/22331>
- Gogikar, P., Tyagi, B. (2016). Assessment of particulate matter variation during 2011–2015 over a tropical station Agra, India. *Atmos. Environ.* 147, 11–21. <https://doi.org/10.1016/J.ATMOSEN.2016.09.063>
- Gogikar, P., Tyagi, B., Padhan, R.R., Mahaling, M. (2018). Particulate matter assessment using in situ observations from 2009 to 2014 over an industrial region of eastern India. *Earth Syst Environ* 2, 305–322. <https://doi.org/10.1007/s41748-018-0072-8>
- Guttikunda, S.K, Gurjar, B.R. (2012). Role of meteorology in seasonality of air pollution in megacity Delhi, India. *Environ. Monit. Assess.* 184, 3199–3211. <https://doi.org/10.1007/s10661-011-2182-8>
- Hagenbjörk, A., Malmqvist, E., Mattisson, K., Sommar, N.J., Modig, L. (2017). The spatial variation of O₃, NO, NO₂ and NO_x and the relation between them in two Swedish cities. *Environ. Monitor. Assess.* 189, 161. <https://doi.org/10.1007/s10661-017-5872-z>
- Hu, Z., Tang, Z., Zheng, C., Guan, M., Shen, J. (2018). Spatial and temporal analyses of air pollutants and meteorological driving forces in Beijing–Tianjin–Hebei region, China. *Environ. Earth Sci.* 77, 540–559. <https://doi.org/10.1007/s12665-018-7705-y>
- Jayamurugan, R., Kumaravel, B., Palanivelraja, S., Chockalingam, M.P. (2013). Influence of temperature, relative humidity and seasonal variability on ambient air quality in a coastal urban area. *Int. J. Atmos. Sci.* 2013, 264046. <https://doi.org/10.1155/2013/264046>
- Karagulian, F., Barbieri, M., Kotsev, A., Spinelle, L., Gerboles, M., Lagler, F., Redon, N., Crunaire, S., Borowiak, A. (2019). Review of the performance of low-cost sensors for air quality monitoring. *Atmosphere*, 10, 506. <https://doi.org/10.3390/atmos10090506>
- Khiem, M., Ooka, R., Hayami, H., Yoshikado, H., Huang, H., Kawamoto, Y. (2010). Process analysis of ozone formation under different weather conditions over the Kanto region of Japan using the MM5/CMAQ modelling system. *Atmos. Environ.* 44, 4463–4473. <https://doi.org/10.1016/j.atmosenv.2010.07.038>
- Kim, E., Hopke, P.K., Edgerton, E.S. (2003). Source identification of Atlanta aerosol by positive matrix factorization. *J. Air Waste Manage. Assoc.* 53, 731–739. <https://doi.org/10.1080/10473289.2003.10466209>
- Kruskal, W.H., Wallis, W.A. (1952). Use of ranks in one-criterion variance analysis. *J. Amer. Stat. Assoc.* 47, 583–621. <https://doi.org/10.2307/2280779>
- Kumar, P., Morawska, L., Martani, C., Biskos, G., Neophytou, M., Di Sabatino, S., Bell, M., Norford, L., Britter, R. (2015). The rise of low-cost sensing for managing air pollution in cities. *Environ. Int.* 75, 199–205. <https://doi.org/10.1016/j.envint.2014.11.019>
- Li, J., Mattewal, S.K., Patel, S., Biswas, P. (2020). Evaluation of nine low-cost-sensor-based particulate matter monitors. *Aerosol Air Qual. Res.* 20, 254–270. <https://doi.org/10.4209/aaqr.2018.12.0485>
- Liu, Y., Yan, C., Ding, X., Wang, X., Fu, Q., Zhao, Q., Zhang, Y., Duan, Y., Qiu, X., Zheng, M. (2017). Sources and spatial distribution of particulate polycyclic aromatic hydrocarbons in Shanghai, China. *Sci. Total Environ.* 584, 307–317. <https://doi.org/10.1016/j.scitotenv.2016.12.134>
- Manikonda, A., Zíková, N., Hopke, P.K., Ferro, A.R. (2016) Laboratory assessment of low-cost PM monitors, *J. Aerosol Sci.* 102, 29–40. <https://doi.org/10.1016/j.jaerosci.2016.08.010>
- Masiol, M., Squizzato, S., Chalupa, D., Rich, D.W., Hopke, P.K. (2018) Evaluation and field calibration of a low-cost ozone monitor at a regulatory urban monitoring station. *Aerosol Air Qual. Res.* 18, 2029–2037. <https://doi.org/10.4209/aaqr.2018.02.0056>
- Mead, M.I., Popoola, O.A.M., Stewart, G.B., Landshoff, P., Calleja, M., Hayes, M., Baldovi, J.J., McLeod, M.W., Hodgson, T.F., Dicks, J., Lewis, A., Cohen, J., Baron, R., Saffell, J.R., Jones, R.L., (2013). The use of electrochemical sensors for monitoring urban air quality in low-cost, high-density networks. *Atmos. Environ.* 70, 186–203. <https://doi.org/10.1016/j.atmosenv.2012.11.060>
- Mohsin, M., Abbas, Q., Zhang, J., Ikram, M., Iqbal, N. (2019). Integrated effect of energy



- consumption, economic development, and population growth on CO₂ based environmental degradation: A case of transport sector. *Environ. Sci. Pollut. Res.* 26, 32824–32835. <https://doi.org/10.1007/s11356-019-06372-8>
- Morais, S., Garcia e Costa, F., de Lourdes Pereira, M. (2012). Heavy Metals and Human Health. in: Oosthuizen, J. (Ed.), *Environmental Health-Emerging Issues and Practice*, Chapter 10. InTech, Rijeka, Croatia, pp. 227–272. <https://doi.org/10.5772/29869>
- Obaseki, D.O., Awopeju, O.F., Awokola, B.I., Adeniyi, B.O., Adefuye, B.O., Ozoh, O.B., Isiguzo, G.C., Amusa, G.A., Adewole, O.O., Erhabor, G.E. (2017). Domestic solid fuel combustion in an adult population in Nigeria: A cross sectional analysis of association with respiratory symptoms, quality of life and lung function. *Respir. Med.* 130, 61–68. <https://doi.org/10.1016/j.rmed.2017.07.014>
- Ogundele, L.T., Owoade, O.K., Olise, F.S., Hopke, P.K. (2016). Source identification and apportionment of PM_{2.5} and PM_{2.5-10} in iron and steel scrap smelting factory environment using PMF, PCFA and UNMIX receptor models. *Environ. Monit. Assess.* 188, 574–594. <https://doi.org/10.1007/s10661-016-5585-8>
- Ogundele, L.T., Owoade, O.K., Hopke, P.K., Olise, F.S. (2017). Heavy metals in industrially emitted particulate matter in Ile-Ife, Nigeria, *Environ. Res.* 156, 320–325. <https://doi.org/10.1016/j.envres.2017.03.051>
- Omokungbe, O.R., Fawole, O.G., Owoade, O.K., Popoola, O.A.M., Jones, R.L., Olise, F.S., Ayoola, M.A., Abiodun, P.O., Toyeye, A.B., Olufemi, A.P., Sunmonu, L.A., Abiye, O.E. (2020). Analysis of the variability of airborne particulate matter with prevailing meteorological conditions across a semi-urban environment using a network of low-cost air quality sensors. *Heliyon* 6, e04207. <https://doi.org/10.1016/j.heliyon.2020.e04207>
- Owoade, O.K., Olise, F.S., Ogundele, L.T., Fawole, O.G., Olaniyi, H.B. (2012). Correlation between particulate matter concentrations and meteorological parameters at a site in Ile-Ife, Nigeria. *Ife J. Sci.* 14, 83–93. <https://doi.org/10.4314/ijcs.v14i1>
- Owoade, K.O., Hopke, P.K., Olise, F.S., Ogundele, L.T., Fawole, O.G., Olaniyi, B.H., Jegede, O.O., Ayoola, M.A., Bashiru, M.I. (2015). Chemical compositions and source identification of particulate matter (PM_{2.5} and PM_{2.5-10}) from a scrap iron and steel smelting industry along the Ife-Ibadan highway, Nigeria. *Atmos. Pollut. Res.* 6, 107–119. <https://doi.org/10.5094/APR.2015.013>
- Owoade, K.O., Hopke, P.K., Olise, F.S., Adewole, O.O., Ogundele, L.T., Fawole, O.G. (2016). Source apportionment analyses for fine (PM_{2.5}) and coarse (PM_{2.5-10}) mode particulate matter (PM) measured in an urban area in southwestern Nigeria. *Atmos. Pollut. Res.* 7, 843–857. <https://doi.org/10.1016/j.apr.2016.04.006>
- Pope, C.A. (2000). Epidemiology of fine particulate air pollution and human health: Biologic mechanisms and who is at risk. *Environ. Health Perspect.* 108, 713–723. <https://doi.org/10.1289/ehp.108-1637679>
- Popoola, O.A.M. (2012). Studies of urban air quality using electrochemical based sensor instruments, Doctoral dissertation, University of Cambridge. <https://doi.org/10.17863/CAM.16288>
- Popoola, O.A.M., Stewart, G.B., Mead, M.I., Jones, R.L. (2016). Development of a baseline temperature correction methodology for electrochemical sensors and its implications for long-term stability. *Atmos. Environ.* 147, 330–343. <https://doi.org/10.1016/j.atmosenv.2016.10.024>
- Popoola, O.A.M., Carruthers, D., Lad, C., Bright, V.B., Mead, M.I., Stettler, M.E.J., Saffell, J.R., Jones, R.L. (2018). Use of networks of low-cost air quality sensors to quantify air quality in urban settings. *Atmos. Environ.* 194, 58–70. <https://doi.org/10.1016/j.atmosenv.2018.09.030>
- RStudio Team (2015). RStudio: Integrated Development for R. RStudio Inc., Boston MA. <http://www.rstudio.com/>
- Seinfeld, J.H., Pandis, S.N. (2016). *Atmospheric Chemistry and Physics: from Air Pollution to Climate Change*, 3rd Ed. John Wiley & Sons, Hoboken, NJ.
- Sousan, S., Koehler, K., Hallett, L., Peters, T.M. (2016). Evaluation of the Alphasense optical particle counter (OPC-N2) and the Grimm portable aerosol spectrometer (PAS-1.108). *Aerosol Sci. Technol.* 50, 1352–1365. <https://doi.org/10.1080/02786826.2016.1232859>
- Sumesh, R.K., Rajeevan, K., Resmi, E.A., Unnikrishnan, C.K. (2017). Particulate matter concentrations in the southern tip of India: Temporal variation, meteorological influences, and source



- identification. *Earth Syst. Environ.* 1, 13–31. <https://doi.org/10.1007/s41748-017-0015-9>
- Tian, G., Qiao, Z., Xu X. (2014). Characteristics of particulate matter (PM₁₀) and its relationship with meteorological factors during 2001-2012 in Beijing. *Environ. Pollut.* 192, 266–274. <https://doi.org/10.1016/j.envpol.2014.04.036>
- Ul-Haq, Z., Tariq, S., Rana, A. D., Ali, M., Mahmood, K., Shahid, P. (2015). Satellite remote sensing of total ozone column (TOC) over Pakistan and neighbouring regions. *Int. J. Remote Sensing* 36, 1038–1054. <https://doi.org/10.1080/01431161.2015.1007255>
- Uria-Tellaetxe, I., Carslaw, D.C. (2014). Conditional bivariate probability function for source identification. *Environ. Modell. Software* 59, 1–9. <https://doi.org/10.1016/j.envsoft.2014.05.002>
- Wang, L., Li, M., Yu, S., Yu, S., Chen, X., Li, Z., Zhang, Y., Jiang, L., Xia, Y., Li, J., Liu, W., Li, P., Lichtfouse, E., Rosenfeld, D., Seinfeld, J.H. (2020). Unexpected rise of ozone in urban and rural areas, and sulfur dioxide in rural areas during the coronavirus city lockdown in Hangzhou, China: Implications for air quality. *Environ. Chem. Lett.* 18, 1713–1723. <https://doi.org/10.1007/s10311-020-01028-3>
- Wang, Y., Munger, J.W., Xu, S., McElroy, M.B., Hao, J., Nielsen, C.P., Ma, H. (2010). CO₂ and its correlation with CO at a rural site near Beijing: Implications for combustion efficiency in China. *Atmos. Chem. Phys.*, 10, 8881–8897. <https://doi.org/10.5194/acp-10-8881-2010>
- Wang, Y., Du, H., Xu, Y., Lu, D., Wang, X., Guo, Z. (2018). Temporal and spatial variation relationship and influence factors on surface urban heat island and ozone pollution in the Yangtze River Delta, China. *Sci. Total Environ.* 631, 921–933. <https://doi.org/10.1016/j.scitotenv.2018.03.050>
- Wilson, J.G., Kingham, S., Pearce, J., Sturman, A. (2005). A review of intraurban variations in particulate air pollution: Implications for epidemiological research. *Atmos. Environ.* 39, 6444–6462. <https://doi.org/10.1016/j.atmosenv.2005.07.030>
- Wongphatarakul, V., Friedlander, S.K., Pinto, J.P. (1998). A comparative study of PM_{2.5} ambient aerosol chemical databases. *Environ. Sci. Technol.* 32, 3926–3934. <https://doi.org/10.1021/es9800582>
- Yashiro, H., Sugawara, S., Sudo, K., Aoki, S., Nakazawa, T. (2009). Temporal and spatial variations of carbon monoxide over the western part of the Pacific Ocean, *J. Geophys. Res.* 114, D08305. <https://doi.org/10.1029/2008JD010876>
- Zhang, Y., Jiang, W. (2018). Pollution characteristics and influencing factors of atmospheric particulate matter (PM_{2.5}) in Chang-Zhu-Tan area. *IOP Conf. Ser.: Earth Environ. Sci.* 108, 042047. <https://doi.org/10.1088/1755-1315/108/4/042047>
- Zikova, N., Masiol, M., Chalupa, D.C., Rich, D.Q., Ferro, A.R., Hopke, P.K. (2017). Estimating hourly concentrations of PM_{2.5} across a metropolitan area using low-cost particle monitors. *Sensors* 17, 1922. <https://doi.org/10.3390/s17081922>